EXPERIMENTAL ASSESSMENT OF 5G-CANDIDATE MODULATION SCHEMES AT EXTREME SPEEDS

José Rodríguez-Piñeiro[1], *Martin Lerch*[2], *Tomás Domínguez-Bolaño*[1],
José A. García-Naya[1], *Sebastian Caban*[2], *and Luis Castedo*[1]
[1]: University of A Coruña, A Coruña, Spain; [2]: TU Wien, Vienna, Austria.
Email: {j.rpineiro, tomas.bolano, jagarcia, luis}@udc.es, {mlerch, scaban}@nt.tuwien.ac.at

ABSTRACT

The radio access technology for railway communications is expected to migrate from GSM for Railways (GSM-R) to fourth generation (4G). Recently, considerable attention has been devoted to high-speed trains since this particular environment poses challenging problems in terms of performance simulation and measurement. In order to considerably decrease the cost and complexity of high-speed measurement campaigns, we have proposed a technique to induce effects caused by highly-time varying channels on multicarrier signals by conducting measurements at low speeds. This technique has been proved to be accurate for the cases of WiMAX and Long Term Evolution (LTE) standardized waveforms. In this work, we evaluate experimentally the performance of this technique by employing modulation schemes proposed for fifth generation (5G) systems. More specifically, we compare the performance obtained by transmitting Filter Bank Multicarrier (FBMC) schemes with two different prototype filters at different velocities in a controlled measurement environment.

1. INTRODUCTION

Over the last few years, broadband communications between nodes moving at high speeds attracted a lot of attention, being the High-Speed Train (HST) modeling one of the most relevant research topics. Nowadays, the dominant technology for the communications between trains and the elements involved in operation, control and intercommunication of the railway infrastructure is GSM for Railways (GSM-R), based on the mature Global System for Mobile Communications (GSM). This technology provides limited capabilities to support advanced services such as automatic pilot applications or provisioning broadband services to the train staff and passengers. Moreover, taking into account the evolution of the general purpose communication standards and devices, fifth generation (5G) systems seem to be good candidates to substitute GSM-R as the basis technology for railway communications in the long term.

One of the most remarkable proposals for the definition of 5G modulation schemes is the utilization of Filter Bank Multicarrier (FBMC) modulation techniques instead of the well-known Orthogonal Frequency-Division Multiplexing (OFDM). FBMC has several advantages for the HST environment, such as *(a)* a higher bandwidth efficiency (allowing for a more efficient utilization of the scarce spectrum available in railway environments while, at the same time, facilitating co-existence with GSM-R), and *(b)* used waveforms can be optimized for doubly dispersive channels like the ones present in HST communications, hence achieving a compromise between the channel response in time and in frequency [7]. Thus, FBMC waveforms were found to perform much better than OFDM for doubly dispersive channels (see [1, 2, 8, 11, 19]).

Some works on techniques for emulation of wireless channels through measurements can be found in the literature, such as [10], where a flexible methodology for over-the-air Multiple-Input, Multiple-Output (MIMO) testing of any baseband equivalent channel realization without requiring channel emulators is proposed. In [9], a flexible broadband MIMO channel measurement methodology was proposed and tested empirically. In our case, in order to dramatically reduce the cost and complexity of high-speed measurement campaigns, we proposed a technique to induce the effects caused by highly time-varying channels in multicarrier signals by conducting the measurements at much lower speeds [17]. This technique consists basically in reducing the subcarrier spacing of the multicarrier signal by scaling down its bandwidth, thus artificially increasing the sensitivity to Inter-Carrier Interference (ICI). Whereas in [17, 20, 21] we considered the transmission of standard-compliant WiMAX Mobile (IEEE 802.16e) signals, in [15] and [16] standard-compliant Long Term Evolution (LTE) signals were used. In [14] we applied the proposed technique to FBMC signals by means of simulations under different channel models at high speeds. In this paper, we empirically validate the obtained results by means of over-the-air measurements.

2. EMULATING HIGH SPEEDS BY TIME INTERPOLATION

Let us consider an FBMC modulation where N_c subcarriers are multiplexed to construct each FBMC symbol. Each FBMC symbol has a total length of N_t samples that are transmitted at a rate $F_s = 1/T_s$. Therefore, each FBMC symbol has a time duration $T_t = T_s N_t$. When an FBMC signal is transmitted, the received signal, namely $r(n)$, can be represented in discrete time as

$$r(n) = \sum_{\tau} h(n, \tau) s(n - \tau) + w(n), \tag{1}$$

where $s(n)$ contains the transmitted FBMC signal, $h(n, \tau)$ is the linear time-variant discrete-time channel impulse response for the sample with index n, and $w(n)$ corresponds to uncorrelated complex-valued white Gaussian noise with variance σ_w^2.

When multicarrier systems are used in time-selective channels, ICI arises in the received signal. The amount of ICI relates to the normalized Doppler spread of the channel, which is given by $D_n = f_d T$, being f_d the maximum Doppler frequency and T the FBMC symbol period, which depends on the FBMC scheme. For example, for Staggered Multitone (SMT) such a symbol period is $T_{\text{SMT}} = T_s N_c/2$.

As proposed in our previous work [17], the parameter T can be adjusted by time interpolation by a factor I, yielding an FBMC symbol period $T^{(I)} = IT$, and consequently an I times narrower

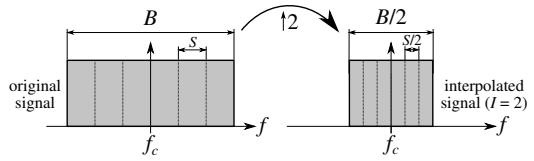

Fig. 1. Example of spectrum compression due to a time interpolation factor $I = 2$. It is straightforward to see that the subcarrier spacing S is also reduced by a factor of $I = 2$ since the total bandwidth B is also reduced by the same factor.

signal bandwidth (see Fig. 1), which leads to a reduced subcarrier spacing (also by a factor of I). Therefore, given the actual velocity v of the mobile receiver, the normalized Doppler spread impacting the time-interpolated FBMC signal can be written as

$$D_n^{(I)} = f_d T^{(I)} = f_d I T = \frac{I T f_c v}{c} = \frac{T f_c}{c} v^{(I)}, \qquad (2)$$

with f_c the carrier frequency, c the speed of light, and $v^{(I)} = Iv$ the emulated speed as a result of an actual measurement speed v and an interpolation factor I. Consequently, enlarging the symbol period $T^{(I)}$ by adjusting I allows for the emulation of a velocity $v^{(I)}$ by conducting measurements at a (presumably much lower) speed v. Note that the statistical properties of the noise do not vary by the decimation process regardless of the interpolation factor.

3. MEASUREMENT SETUP AND PROCEDURE

3.1. Evaluation Setup

We use the evaluation setup shown in Fig. 2 to test the technique of emulating high speeds by time interpolation of FBMC signals. The setup consists of the blocks explained below.

3.1.1. Signal generation (transmitter side) and signal processing (receiver side)

At the transmitter side, signals are generated using a custom-developed FBMC/OFDM signal generator. Two different prototype filters were implemented for the FBMC case, namely the one defined by the PHYDYAS project [3] and the so-called Hermite pulse [11], being the latter suited for transmissions over doubly dispersive channels [11]. At the receiver side, a custom-developed FBMC receiver is used, which includes basic algorithms for channel estimation, interpolation and equalization, as well as time and frequency synchronization. Regarding the channel equalization, a Zero-Forcing (ZF) strategy was considered. Several so-called auxiliary pilot schemes were implemented [6, 12, 18] to deal with the interference caused by the lack of orthogonality of the received symbols when FBMC signals are transmitted. For the results shown in this paper, the so-called Coded Auxiliary Pilot (CAP) method [6] (using 8 symbols around each pilot) was considered.

3.1.2. Time interpolation and time decimation

the signal is time-interpolated by a factor I at the transmitter and decimated by the same factor I at the receiver side. This way we emulate a Doppler spread similar to that obtained with a speed increase by the factor of I.

3.1.3. Signal transmission and reception under actual high-speed conditions

signals are transmitted over the air by using a testbed developed at the TU Wien [13]. The testbed transmitter is placed outdoors on a roof of a building in downtown Vienna, Austria. The receiver is placed indoors in an adjacent building at a distance of 150 meters. While the transmit antenna is fixed, the receive antenna is rotated around a central pivot in a controlled and repeatable way [5], recreating an infrastructure to vehicle scenario. Note that the trajectory of the antenna is well approximated as a transversal movement for sufficiently short transmissions. Notice also that the testbed is equipped with a highly precise time and frequency synchronization system based on Global Positioning System (GPS)-disciplined rubidium oscillators and a custom-made synchronization unit [4]. As a result, we can assume that the results are not affected by time or frequency offsets due to imperfect synchronization.

3.2. Evaluation Procedure

In order to evaluate the impact of high-speed conditions on FBMC transmissions, actual receiver velocities ranging from 50 km/h to 400 km/h were considered. Furthermore, interpolation factors of $I = 1$ (no interpolation), $I = 2$, and $I = 3$ were used to emulate velocities ranging from 50 km/h to 1200 km/h. Note that it is possible to emulate the same speed (i.e., generate the same Doppler spread value) from different combinations of the actual measurement velocity and the interpolation factor (see Table 1), thus we emulated the same speed by means of different actual receiver speeds and interpolation factors and then we compared the obtained results.

Several measurements were conducted for each velocity and interpolation factor. More concretely, the whole receiver (including the antenna rotation unit) was moved in two dimensions on the floor among 16 different positions. For each receiver position, 6 measurements per velocity and interpolation factor were carried out, each starting at a given angular-shift on the circumference defined by the receive rotating antenna. We always transmitted the same set of symbols (including data and pilots) for each modulation scheme, hence enabling a fair comparison of the results of different measurements.

To be able to compare the results gathered from different interpolation factors, we consider the following aspects:

3.2.1. Equal receive antenna trajectory

the trajectory of the receive antenna during the transmission of each of the signals does not vary if the emulated speed is kept constant. The arc length defined by the antenna during the transmission of a single FBMC symbol, namely ΔZ, can be expressed as $\Delta Z = \left(v^{(I)}/I\right) T_t I$, where $v = v^{(I)}/I$ is the actual rotation speed and $T_t I$ is the time required for transmitting an FBMC symbol after being interpolated by a factor of I. It can be seen that ΔZ does not vary regardless of the interpolation factor I.

3.2.2. Equal average transmit energy per symbol

in order to preserve the average energy per symbol, the interpolated signals are scaled down in amplitude by a factor of $\sqrt{I}$ before being transmitted.

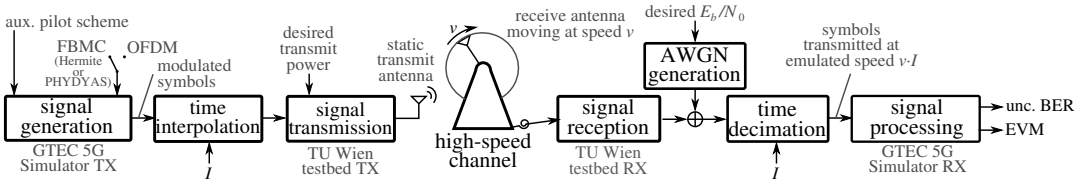

Fig. 2. Block diagram of the setup used for the evaluations.

Table 1. Combinations of actual velocities and interpolation factors employed in the measurements.

	interpolation factors $I \in \{1$ (no interpolation), $2, 3\}$													
	emulated velocity [km/h]													
actual velocity [km/h]	50	66.6	100	133.3	150	200	266.6	300	400	450	600	800	900	1200
50	1	–	2	–	3	–	–	–	–	–	–	–	–	–
66.6	–	1	–	2	–	3	–	–	–	–	–	–	–	–
100	–	–	1	–	–	2	–	3	–	–	–	–	–	–
133.3	–	–	–	1	–	–	2	–	3	–	–	–	–	–
150	–	–	–	–	1	–	–	2	–	3	–	–	–	–
200	–	–	–	–	–	1	–	–	2	–	3	–	–	–
300	–	–	–	–	–	–	–	1	–	–	2	–	3	–
400	–	–	–	–	–	–	–	–	1	–	–	2	–	3

3.2.3. Ensuring a fair OFDM vs FBMC comparison

in order to be able to fairly compare the results for the different considered modulation schemes (OFDM and FBMC with Hermite and PHYDYAS prototype filters), the same number of subcarriers, as well as the same subcarrier spacing, was considered for all cases. Also the same algorithms for channel estimation, interpolation and equalization were employed for all modulation schemes. The pilot density was kept constant for all cases. A 2-PAM constellation is used for the FBMC transmissions, whereas 4-QAM is considered for OFDM, since the symbols are complex-valued in the latter case. Finally, the signals are scaled to ensure that the transmitted energy per bit is equivalent for both OFDM and FBMC. As a consequence of most of the aforementioned aspects, the user bit rate is approximately the same for OFDM and FBMC, being the slight differences caused by the overhead inherent to the use of the Auxiliary Pilots (APs) required in FBMC [6], the OFDM cyclic prefix and the time dispersion of the prototype filters in FBMC. Table 2 details the most relevant parameters used for the measurements.

Note that the number of used subcarriers could be increased in FBMC with respect to OFDM for a fixed spectral mask as the subcarriers are better frequency-localized. Furthermore, we could also increase the bandwidth per subcarrier, i.e., decrease the number of subcarriers while keeping the total used bandwidth constant for FBMC. Although this would require more advanced equalizers, it will be beneficial in terms of Peak-to-Average Power Ratio (PAPR). However, to perform a fair comparison, we decided to keep both the number of subcarriers as well as the subcarrier spacing constant, although this implies not to take advantage of all the potential benefits of FBMC systems.

4. OBTAINED RESULTS

We consider two figures of merit: *(a)* the uncoded BER, which is calculated as the BER after the hard symbol decision and it is one of the most used performance metrics in wireless communications and *(b)* the EVM, an unbounded and continuous metric particularly valuable when the Signal-to-Noise Ratio (SNR) is high enough to saturate the BER to its minimum value of zero. All the included results are expressed in terms of the two aforementioned figures of merit with respect to E_b/N_0 or the receiver speed (actual receiver speed for $I = 1$ and emulated speed in other cases). With the purpose of gauging the accuracy of the results, 95% confidence intervals are also included.

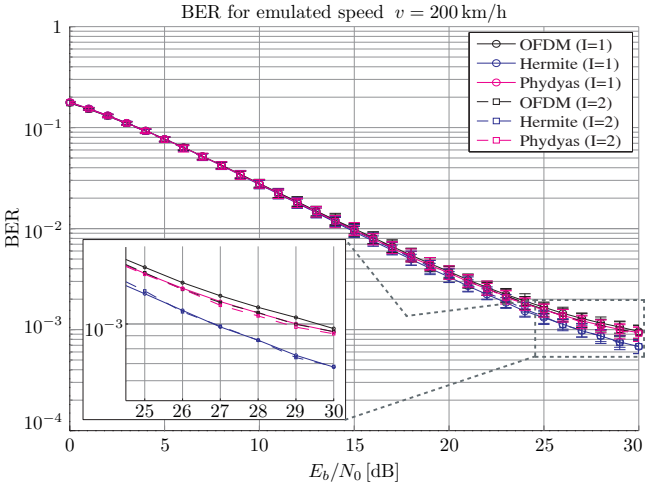

Fig. 3. Uncoded BER versus E_b/N_0 for different modulation schemes and interpolation factors.

Figure 3 shows the BER versus E_b/N_0 for an emulated speed of 200 km/h for the interpolation factors $I = 1$ (i.e., no interpolation) and $I = 2$ and all the modulation schemes considered. It can be seen that the curves for each modulation almost overlap regardless of the interpolation factor. Moreover, the performance is very similar when the emulated speed is 200 km/h for all modulation schemes. Only slight differences can be observed for very high E_b/N_0 values, since the random effects due to noise are minimized and hence do not hide other sources of disagreement in the results. Note that, in these cases, FBMC with the Hermite prototype filter

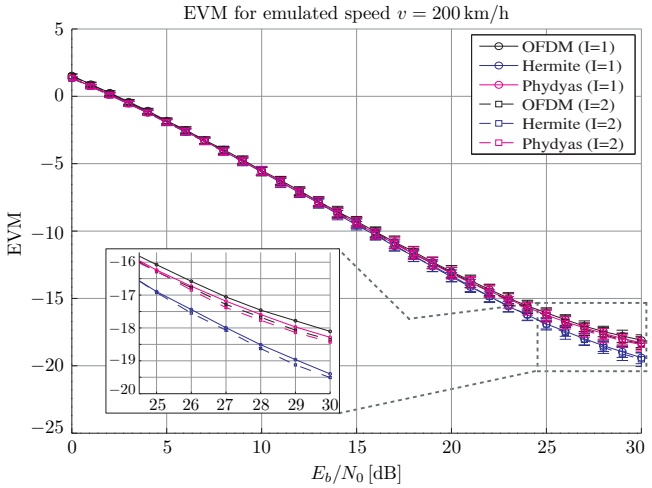

Fig. 4. EVM versus E_b/N_0 for different modulation schemes and interpolation factors.

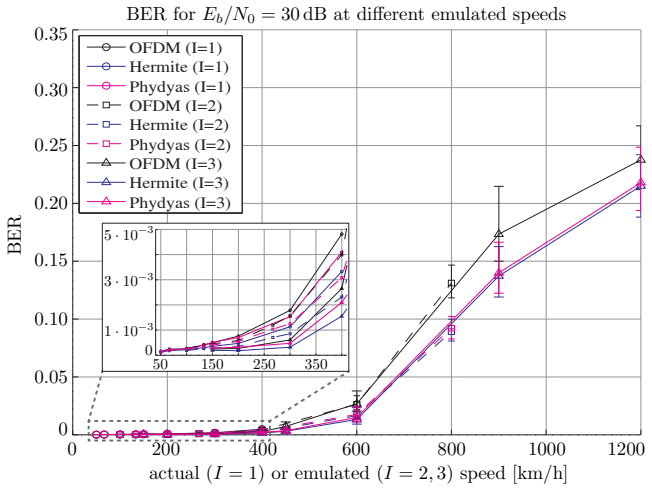

Fig. 5. Uncoded BER versus receiver speed for different modulation schemes and interpolation factors.

performs a bit better than the other alternatives. Figure 4 shows the performance in terms of EVM for an emulated speed of 200 km/h and $I = 1, 2$. It can be seen that the obtained results are strongly correlated with those corresponding to BER. Moreover, the curves also overlap regardless of the interpolation factor, showing that the proposed technique is also well suited to emulate the distortion suffered by the received constellations due to the movement of the receiver. In the remaining of this section we consider $E_b/N_0 = 30\,\text{dB}$ as the worst case for the proposed technique.

Figure 5 shows the BER versus the emulated speed for $I = 1, 2, 3$ and all the modulation schemes being considered. On the one hand, curves corresponding to different interpolation factors show an excellent level of agreement for each of the modulation schemes. A significant difference on the performance between OFDM and FBMC (for both considered prototype filters) can be observed for speeds higher than 400 km/h. It should be taken into account that both considered prototype filters for FBMC are much better localized in frequency than the OFDM waveform, hence they account better for the time dispersion of the channel. In other words, they

Table 2. Main parameters used in the experiments.

Parameter	Value
Sampling frequency, F_s	15.36 MHz
FFT size	1024 points
Number of used subcarriers	600 (excluding DC)
CP length (OFDM)	72 samples
Constellations	2-PAM (FBMC) 4-QAM (OFDM)
Pilot spacing	8 subcarriers (frequency dimension) 10 symbols (time dimension, FBMC) 5 symbols (time dimension, OFDM)
AP scheme	CAP (8 surrounding symbols)
Pulse overlapping	3 symbols (Hermite) 4 symbols (PHYDYAS)
Actual velocities, v	50, 66.6, 100, 133.3, 150, 200, 300, and 400 km/h
Carrier frequency, f_c	2.5 GHz
Interpolation factors, I	1, 2, and 3
E_b/N_0	from 0 to 30 dB

are better suited to combat the ICI. However, for practical HST speeds (less than 350 km/h), the difference is not very significant. Still a slight difference in the results obtained for the PHYDYAS and Hermite prototype filters can be observed, being the better results obtained for the latter one. The reason for this behavior is that the Hermite prototype filter is slightly worse localized in frequency than the PHYDYAS one, but it is better localized in time.

5. CONCLUSIONS

In this paper we evaluate empirically a technique to induce the effects caused by highly time-varying channels in multicarrier signals by conducting the measurements at low speeds in a controlled environment by transmitting FBMC-modulated signals.

According to the results, FBMC can be a much convenient choice (in terms of BER performance) than OFDM for very high speeds (400 km/h or more) when adequate prototype filters are used (e.g., the so-called Hermite pulse). For practical HST velocities the difference is not very significant. However, the results show that the potential advantages of FBMC for HST environments, such as the higher bandwidth efficiency, could be exploited without additional performance losses.

From the excellent level of agreement of the results obtained for different interpolation factors as well as without interpolation, it can be concluded that the proposed technique is valid for inducing high-speed effects in FBMC-based systems.

Finally, the obtained results corroborate empirically those previously shown in [14] by means of simulations.

ACKNOWLEDGMENT

This work has been funded by the Christian Doppler Laboratory for Wireless Technologies for Sustainable Mobility, KATHREIN Werke KG, A1 Telekom Austria AG, Xunta de Galicia, MINECO of Spain, and FEDER funds of the EU under grants with numbers 2012/287, TEC2013-47141-C4-1-R, FPU12/04139, EST14/00355, and BES-2014-069772. The financial support by the Austrian Federal Ministry of Economy, Family and Youth and the National Foundation for Research, Technology and Development is gratefully acknowledged.

6. REFERENCES

[1] M. Alard. Construction of a multicarrier signal, Aug. 21 2001. US Patent 6,278,686.

[2] P. Amini, C. H. Yuen, R.-R. Chen, and B. Farhang-Boroujeny. Isotropic filter design for MIMO filter bank multicarrier communications. In *IEEE Sensor Array and Multichannel Signal Processing Workshop (SAM)*, pages 89–92, 2010.

[3] M. Bellanger, D. Le Ruyet, D. Roviras, M. Terré, J. Nossek, L. Baltar, Q. Bai, D. Waldhauser, M. Renfors, T. Ihalainen, et al. FBMC physical layer: a primer. Technical report, PHYDYAS FP7 Project Document, 2010.

[4] S. Caban, A. Disslbacher-Fink, J. A. Garcia-Naya, and M. Rupp. Synchronization of wireless radio testbed measurements. In *Proc. International Instrumentation and Measurement Technology Conference (I2MTC 2011)*, Binjiang, Hangzhou, China, May 2011.

[5] S. Caban, J. Rodas, and J. Garcia-Naya. A methodology for repeatable, off-line, closed-loop wireless communication system measurements at very high velocities of up to 560 km/h. In *2011 IEEE Instrumentation and Measurement Technology Conference*, pages 1–5, May 2011.

[6] W. Cui, D. Qu, T. Jiang, and B. Farhang-Boroujeny. Coded auxiliary pilots for channel estimation in FBMC-OQAM systems. *IEEE Transactions on Vehicular Technology*, PP(99):1–1, 2015.

[7] B. Farhang-Boroujeny. OFDM versus filter bank multicarrier. *IEEE Signal Processing Magazine*, 28(3):92–112, 2011.

[8] B. L. Floch, M. Alard, and C. Berrou. Coded orthogonal frequency division multiplex [tv broadcasting]. *Proceedings of the IEEE*, 83(6):982–996, 1995.

[9] J. Gutiérrez, Ó. González, J. Pérez, D. Ramírez, L. Vielva, J. Ibáñez, and I. Santamaría. Frequency-domain methodology for measuring MIMO channels using a generic test bed. *IEEE Transactions on Instrumentation and Measurement*, 60(3):827–838, March 2011.

[10] J. Gutiérrez, J. Ibáñez, and J. Pérez. Mimo ota testing based on transmit signal processing. *Hindawi International Journal of Antennas and Propagation*, May 2013.

[11] R. Haas and J.-C. Belfiore. A time-frequency well-localized pulse for multiple carrier transmission. *Wireless Personal Communications*, 5(1):1–18, 1997.

[12] J.-P. Javaudin, D. Lacroix, and A. Rouxel. Pilot-aided channel estimation for OFDM/OQAM. In *57th IEEE Semiannual Vehicular Technology Conference (VTC 2003-Spring)*, volume 3, pages 1581–1585, 2003.

[13] M. Lerch, S. Caban, M. Mayer, and M. Rupp. The Vienna MIMO testbed: Evaluation of future mobile communication techniques. *Intel Technology Journal*, 18(3):58–69, 2014.

[14] J. Rodríguez-Piñeiro, T. Domínguez-Bolaño, P. Suárez-Casal, J. A. García-Naya, and L. C. Ribas. Affordable evaluation of 5G modulation schemes in high speed train scenarios. In *ITG Workshop on Smart Antennas (WSA 2016)*, Munich, Germany, March 2016. Accepted for publication.

[15] J. Rodríguez-Piñeiro, M. Lerch, J. A. García-Naya, S. Caban, M. Rupp, and L. Castedo. Emulating extreme velocities of mobile LTE receivers in the downlink. *EURASIP Journal on Wireless Communications and Networking*, 2015(106), April 2015.

[16] J. Rodríguez-Piñeiro, M. Lerch, P. Suárez-Casal, J. A. García-Naya, S. Caban, M. Rupp, and L. Castedo. LTE downlink performance in high speed trains. In *2015 IEEE 81st Vehicular Technology Conference (VTC2015-Spring)*, Glasgow, United Kingdom, May 2015.

[17] J. Rodríguez-Piñeiro, P. Suárez-Casal, J. A. García-Naya, L. Castedo, C. Briso-Rodríguez, and J. I. Alonso-Montes. Experimental validation of ICI-aware OFDM receivers under time-varying conditions. In *IEEE 8th Sensor Array and Multichannel Signal Processing Workshop (SAM 2014)*, A Coruña, Spain, June 2014.

[18] T. H. Stitz, T. Ihalainen, A. Viholainen, and M. Renfors. Pilot-based synchronization and equalization in filter bank multicarrier communications. *EURASIP Journal on Advances in Signal Processing*, 2010:9, 2010.

[19] T. Strohmer and S. Beaver. Optimal OFDM design for time-frequency dispersive channels. *IEEE Transactions on Communications*, 51(7):1111–1122, 2003.

[20] P. Suárez-Casal, J. Rodríguez-Piñeiro, J. A. García-Naya, and L. Castedo. Experimental evaluation of the WiMAX downlink physical layer in high-mobility scenarios. *EURASIP Journal on Wireless Communications and Networking*, 2015(109), Decemeber 2014.

[21] P. Suárez-Casal, J. Rodríguez-Piñeiro, J. A. García-Naya, L. Castedo, C. Briso-Rodríguez, and J. I. Alonso-Montes. Experimental assessment of WiMAX transmissions under highly time-varying channels. In *Eleventh International Symposium on Wireless Communication Systems (ISWCS)*, pages 717–721, Barcelona, Spain, August 2014.